Journal for ImmunoTherapy of Cancer

Liquid biopsy approach to monitor the efficacy and response to CAR-T cell therapy

Stephanie N Shishido,[1] Olivia Hart,[1] Sujin Jeong,[1] Aidan Moriarty,[1] Darren Heeke,[2] John Rossi,[2] Adrian Bot,[2] Peter Kuhn [1,3,4,5,6,7]

To cite: Shishido SN, Hart O, Jeong S, *et al*. Liquid biopsy approach to monitor the efficacy and response to CAR-T cell therapy. *Journal for ImmunoTherapy of Cancer* 2024;**12**:e007329. doi:10.1136/jitc-2023-007329

► Additional supplemental material is published online only. To view, please visit the journal online (https://doi.org/10.1136/jitc-2023-007329).

Accepted 25 January 2024

For numbered affiliations see end of article.

Correspondence to
Dr Peter Kuhn; pkuhn@usc.edu

ABSTRACT

Background Chimeric antigen receptor (CAR)-T cells are approved for use in the treatment of hematological malignancies. Axicabtagene ciloleucel (YESCARTA) and brexucabtagene autoleucel (TECARTUS) genetically modified autologous T cells expressing an anti-CD19 scFv based on the FMC63 clone have shown impressive response rates for the treatment of CD19+B cell malignancies, but there remain challenges in monitoring long-term persistence as well as the functional characterization of low-level persisting CAR-T cells in patients. Furthermore, due to CD19-negative driven relapse, having the capability to monitor patients with simultaneous detection of the B cell malignancy and persisting CAR-T cells in patient peripheral blood is important for ensuring timely treatment optionality and understanding relapse.

Methods This study demonstrates the development and technical validation of a comprehensive liquid biopsy, high-definition single cell assay (HDSCA)-HemeCAR for (1) KTE-X19 CAR-T cell identification and analysis and (2) simultaneously monitoring the CD19-epitope landscape on neoplastic B cells in cryopreserved or fresh peripheral blood. Proprietary anti-CD19 CAR reagents, healthy donor transduced CAR-T cells, and patient samples consisting of malignant B cell fractions from manufacturing were used for assay development.

Results The CAR-T assay showed an approximate limit of detection at 1 cell in 3 million with a sensitivity of 91%. Genomic analysis was additionally used to confirm the presence of the CAR transgene. This study additionally reports the successful completion of two B cell assays with multiple CD19 variants (FMC63 and LE-CD19) and a unique fourth channel biomarker (CD20 or CD22). In patient samples, we observed that CD19 isoforms were highly heterogeneous both intrapatient and interpatient.

Conclusions With the simultaneous detection of the CAR-T cells and the B cell malignancy in patient peripheral blood, the HDSCA-HemeCAR workflow may be considered for risk monitoring and patient management.

WHAT IS ALREADY KNOWN ON THIS TOPIC

⇒ Monitoring ongoing responses and assessing the risk of relapse are novel challenges when addressing the long-term needs of patients treated with CAR-T cell therapy. The detection of circulating CAR-T cells in blood samples is currently conducted via flow cytometry or quantitative PCR. These methodologies have limitations in detection sensitivity and single cell analysis capabilities.

WHAT THIS STUDY ADDS

⇒ A comprehensive liquid biopsy approach can simultaneously detect the B cell malignancy and persisting CAR-T cells with high sensitivity at the molecular level in patient peripheral blood. The reproducibility and robustness of the IF assays developed and validated here with a semiquantitative characterization of each cell is critical for our understanding of treatment efficacy and further downstream molecular analysis.

HOW THIS STUDY MIGHT AFFECT RESEARCH, PRACTICE OR POLICY

⇒ A liquid biopsy can be used to maximize our understanding of therapeutic success or failure and future patient management. Routine monitoring of CAR-T cell populations via a comprehensive liquid biopsy may provide insight into the quality, heterogeneity, and persistence of CAR-T cells in circulation, while allowing for association with the occurrence of toxic events. The understanding of the CD19 landscape on the malignant B cells can provide insight into treatment efficacy and resistance.

BACKGROUND

Chimeric antigen receptor (CAR)-T cells have been approved for use in the treatment of hematological malignancies. Theranostic approaches are required to help predict efficacy and monitor response in individual patients. Current strategies used to identify the presence of CAR-T cells in blood or bone marrow rely on quantitative PCR (qPCR) and minimalistic flow cytometry antibody panels.[1–4] Due to limiting cell numbers at time points beyond 1-month postinfusion,[5 6] little is known about whether the persisting gene marked CAR-T cells are functional in terms of surface CAR expression, phenotype, proliferative index, and other aspects of immune function such as expression of exhaustion markers that may associate with

durable response, prolonged B cell aplasia, or disease relapse. The CAR-T field's current understanding of clinical efficacy reflects a general observation that the magnitude of CAR-T expansion in peripheral blood (PB), within 2 weeks post-treatment, correlates with objective response and toxicity.[4 7–9] A central question is functional relevance of long-term persisting CAR-T cells in patients with ongoing complete response (CR) or durable partial response (PR). To date, few studies have done a phenotypic characterization of persisting CAR-T cells in which an association with persisting CAR-T cells and clinical outcome was revealed.[10]

Genetically modified autologous T cells expressing an anti-CD19 CAR based on the FMC63 clone have shown impressive response rates for the treatment of CD19+B cell malignancies.[2 9 11–14] However, in acute lymphoblastic leukemia (ALL), 30%–60% of patients relapse after anti-CD19 CAR treatment, of which up to 20% are CD19-negative relapse.[15] Similarly, up to 30% of secondary treatment failures in diffuse large B cell lymphoma patients treated with axicabtagene ciloleucel show greatly diminished or absent CD19 tumor expression at relapse.[16] However, owing to the nature of the reagents used, the analysis, to date, may have underestimated the true rate of target related evasion. Engineered T cell persistence does not prevent CD19-negative relapse, while single-target therapy may further lead to escape variants including target isoforms devoid of cognate epitope (FMC63) owing to alternate splicing, exon skipping or other mechanisms.[17] Therefore, monitoring the CD19 landscape at the epitope level in the heterogeneous B cell population, is important for ensuring treatment efficacy and understanding relapse with CD19 negative disease or FMC63 evasion due to aberrations in CD19 expression that emerge under selective pressure. Improving early detection of malignant cells and understanding the underlying mechanisms of treatment escape can lead to both scientific discovery for next generation CAR-T designs and immediate line of sight to clinical impact.

This study uses the high-definition single cell assay (HDSCA) platform[18 19] for rare event detection from liquid biopsy. By design, the HDSCA platform uses minimally processed blood samples in an enrichment-free, direct imaging, high-throughput computational analysis approach to identify rare cells and characterize them at the cellular, protein, and molecular level developed at Scripps Research and USC, and licensed to Epic Sciences for commercial development.[20–22] The HDSCA platform maintains a complete chain of custody from the patient data to the bulk sample to the individual analyte. The rare cell identification part of the platform is extensively validated in both the research use only and clinical laboratory improvement amendments certified setting. Methods have been extensively described in the literature[23–26] and routinely used for the detection of circulating tumor cells (CTCs) in human blood samples while collecting over 700 morphometric parameters which represent size, shape, signal intensity, and other morphological features of the single cells.[18 19 27–29] The HDSCA platform is well suited to providing high content data sets to characterize CAR-T cells, the B cell CD19 landscape, as well as the normal leucocyte population from liquid biopsies.

Here, the HDSCA platform will be used in the context of B cell malignancies, particularly ALL and mantle cell lymphoma being treated with KTE-X19 CAR-T cells. This study was focused on the technical development and validation of (1) a rare cell identification assay to detect and analyze KTE-X19 CAR-T cells and (2) a B cell assay to monitor the epitope landscape on neoplastic B cells in cryopreserved or fresh PB. The resulting HDSCA-HemeCAR workflow is designed to analyze select biospecimens collected from patients treated with genetically engineered T cells, to aid in our understanding of persisting anti-CD19 CAR-T cells while simultaneously (from the same specimen) monitoring the disease derived cells.

METHODS

Antibodies, cell lines, human samples

Proprietary anti-CD19 CAR reagents and healthy donor transduced cells were provided by Kite Pharma for assay development: KIP-1 (16-6) rabbit mAb, KIP-3 (14-1) rabbit mAb, and CDL (anti-FMC63 scFv) mouse mAb. Commercially available antibodies include anti-human CD20 clone 2H7 mouse IgG2bk (Biolegend, 302302), anti-human CD22 clone S-HCL-1 mouse IgG2b (Biolegend, 363502), anti-human CD19 clone FMC63 mouse IgG2a (Sigma-Aldrich, MAB1794), anti-human CD19 clone LE-CD19 mouse IgG1 (Dako, GA65661-2), anti-human CD3 clone UCHT1 direct conjugate to Alexa Flour 647 mouse IgG1 (Biolegend, 300416).

Lab manufactured CAR-T cells and cell lines were used to develop HDSCA-HemeCAR. SU-DHL-4 (CRL-2957) and Jurkat (E6-1; TIB-152) cell lines were purchased from ATCC. Normal donor (ND) PB was procured from Scripps Normal Blood Donor Service.

ZUMA-3 (NCT02614066) cryopreserved PB mononuclear cells (PBMCs) from the negative manufacturing fraction were provided by Kite Pharma. The negative fraction is the subset of cells from leukapheresis that are not used for manufacturing the CAR-T cells and thus contain the B cell malignant cellular population prior to therapy. ZUMA-3 is a pivotal phase 1/2 study evaluating KTE-X19 autologous anti-CD19 CAR-T cell therapy in adult relapsed/refractory (R/R) B-ALL. Patient clinical data were limited to type of response each individual presented with after KTE-X19 CAR-T cell therapy.

Sample preparation and blood processing

ND samples were processed as previously described.[23] Briefly, after red blood cell lysis, control cell line cells were spiked into the sample (10%) and nucleated cells were plated as a monolayer of ~3 million cells per 1-well slide and 40,000 cells per well on 12-well slides (Marienfeld, Lauda, Germany) followed by cryobanking at −80°C.

CAR-T cell assay limit of detection (LOD) sample preparations were made using varying numbers of CAR-T cells (0, 4, 20, 50, 100) from serial dilutions to the 1-well slide format to observe the rate of detection. Cryopreserved patient samples were thawed in 37°C water batch, swirling constantly, followed by a PBS rinse prior to plating on 1-well slides at ~3 million cells per slide. Cell count was taken using an automated blood cell counter (Medonic M-series).

Immunofluorescent assay validation

Two immunofluorescent (IF) assays were designed and validated as part of HDSCA-HemeCAR. The first was the CAR-T Assay, which consists of nuclei detection via DAPI, use of a CAR detecting proprietary antibody, anti-CD19 (FMC63), and anti-CD3 (UCHT1). The second was the B Cell Assay, which included nuclei detection via DAPI, anti-CD19 (FMC63), anti-CD19 (LE-CD19), and either anti-CD20 (2H7) or anti-CD22 (S-HCL-1).

Contrived samples were used to confirm performance accuracy and reproducibility of IF assays. Samples were fixed with 2% neutral buffered formalin solution (VWR, San Dimas, California, USA) for 20 min. Non-specific binding sites were blocked with 10% goat serum (Millipore, Billerica, Massachusetts, USA) for 20 min. Primary antibody and fluorescently labeled secondary antibody titration experiments were conducted on 12-well slides to find optimal concentrations under HDSCA platform conditions. Specificity of CAR targeting reagents (primary mAb and secondary mAb) were estimated in anti-CD19 CAR-T cell negative samples including ND cells that do not contain the antigen recognized by Kite's proprietary antibody. Specificity of B cell targeting reagents (primary mAb and secondary mAb) were estimated in B cell positive control cell line (SU-DHL-4) and T cell negative control cell line (Jurkat) which does not contain the CD19 antigen.

For patient samples, slides were stained with the optimized IF protocol. Since cryopreserved PBMCs are not the typical sample received for HDSCA processing and analysis, the B cell assay was performed on freshly plated slides to minimize potential epitope changes from repeated cryopreservation.

Imaging

Automated scanning of slides was conducted using a custom high-throughput fluorescence scanning microscope collecting 2304 frames per slide at ×100 magnification with exposures and gain set to yield constant background intensity level for normalization purposes.[18 23 25] Candidate cells of interest were further imaged manually at ×200 or ×400 magnification. For assay optimization, triplicate slides were used per condition, three regions of interest per slide were imaged, and all cells in the ROI were analyzed in CellProfiler (V.4.2.1) for the signal of interest.

Rare event detection

The rare event detection algorithm (OCULAR) used here has been previously published.[18 19] In brief, all cells were segmented to generate nuclear and/or cytoplasm masks for feature extraction, which was followed by a dimensionality reduction using principal components and hierarchical clustering to separate common cells (mainly white cell count, WCC) and rare cells in each image frame. Importantly, the algorithmic approach does not depend on specific markers and is fully compatible with all IF protocols including the CAR-T IF assay. The OCULAR methodology was used to classify rare cells into eight distinct channel types based on the fluorescence image intensity of four markers DAPI|Alexa Fluor 488|Alexa Fluor 555|Alexa Fluor 647 to assist in optimization and validation of the IF assays with the detection of different cellular populations. Further rare CAR-T or B cell phenotype evaluations were conducted manually based on biomarker expression in four fluorescence channels for each IF protocol.

LOD analysis

The LOD samples were stained with the optimized CAR-T assay protocol, slides imaged at ×100 magnification using automated scanning, and rare cells identified using the OCULAR algorithm. Single cells identified as CDL+CD3+ were isolated for confirmation of the CAR transgene. Additional cells were isolated as controls to confirm the lack of the CAR transgene. The nested PCR (nPCR) methodology optimization is discussed below. This test was used to show the sensitivity of the CAR-T cell assay at 1 in 3 million cells which is equivalent to 1 cell in 0.5–1 mL of blood, showing an increased sensitivity over current alternative detection approached.

Single cell isolation for genomics

Identified CAR-T and WCC were isolated for genomic analysis at the single cell level as described previously.[25 26 30] Briefly, a glass microcapillary (Piezo Drill Tip, Eppendorf) was inserted into the micromanipulation arm of an Eppendorf Transfer Man NK2 micromanipulator (Eppendorf AG, Hamburg, Germany) and used to transfer each cell of interest to a sterile 0.5 mL PCR tube containing 1 µL of TE buffer (10 mM Tris-HCl+1 mM EDTA pH 8.0). PCR tubes containing single cells were flash frozen and stored at −80°C with an aliquot of the TE buffer for use as a control in all downstream genomic processing.

PCR primer design

Primer pairs were designed against a specific region unique to the CAR transgene sequence: the "outer" primer pair targeting a 717-base pair (bp) region (CAR outer) and the "inner" primer pair targeting a 116 bp region (CAR inner). Primer pairs to detect short tandem repeats (STRs) were designed for use as an internal control amplicon for cellular material due to the prevalence of STRs in the genome. We identified three STR primer pairs from a published paper[31] to test with our methodology and HDSCA prepared samples. Primer sequences are provided in table 1.

Table 1 Primer sets used for nPCR for CAR transgene detection at the single cell level

Primer name		Sequence	Tm (°C)	Product size (bp)
STR1 (chr5)	Forward	TTGCAGGAAATGCTGGCATAGAGC	68.5	486
	Reverse	TTCTGTAACATTTTGCCACATACGCC	66.8	
STR2 (chr5)	Forward	TGCAGCCTAATAATTGTTTTCTTTGGG	66	291
	Reverse	AGATTCACTTTCATAATGCTGGCAGA	64.3	
STR3 (chrY)	Forward	ACCACTGTACTGACTGTGATTACAC	57.3	495
	Reverse	GCACCTCTTTGGTATCTGAGAAAGT	61.3	
CAR (outer)	Forward	TCAGGGGTCTCATTACCCGA	57.4	717
	Reverse	ATCGTACTCCTCTCTTCGTCCT	56.6	
CAR (inner)	Forward	GCCATTTACTACTGTGCCAAAC	54.5	116
	Reverse	GGATACATAACTTCAATTGCGGC	54.5	

nPCR, nested PCR.

nPCR for single CAR-T cell detection

Validation of CAR-T IF assay was conducted through detection of the CAR at the single cell level using a multiplex nPCR approach. An nPCR protocol was developed to coamplify the FMC63-CD28-CD3ζ transgene of transduced KTE-C19 (Yescarta) cells and STR regions used as controls. Single cells were first lysed at 95°C for 2 min by adding 1.5 µL of 100 mM DTT and 400 mM KOH lysis buffer, followed by genomic fragmentation using 8.5 µL of 18:1 10 mM Tris and Proteinase K buffer solution and incubating at 50°C for 1 hour, 80°C for 20 min, and 99°C for 4 min. Positive controls consisted of 1 µL of bulk CAR+cells obtained from Kite Pharma and negative controls consisted of 1 µL bulk WCC from ND samples run through the HDSCA-HemeCAR workflow.

The first round PCR reactions (outer amplification step) were performed in a final reaction volume of 25 µL with a reaction mix consisting of 10.5 µL digested DNA template, 12.5 µL 2× OneTaq Hot Start Master Mix (NEB #M0489S), 0.2 µM forward and reverse STR primers, and 0.4 µm forward and reverse outer CAR primers. The amplification conditions were initial denaturing at 94°C for 1 min, followed by 35 cycles of denaturing at 94°C for 25 s, annealing at 58°C for 40 s, extension at 68°C for 50 s, and after all 35 cycles are complete an additional extension phase at 68°C for 5 min.

The second round of PCR reactions (inner amplification step) were performed in a reaction volume of 25 µL with a reaction mix consisting of 1 µL template PCR product from the outer amplification step, 6:1 ratio of 2× OneTaq Hot Start Master Mix to the total volume of primers per reaction, DNAse-free water, and either 0.2 µM forward and reverse STR primers or 0.3 µM forward and reverse inner CAR primers. Unlike the outer amplification step, inner amplification PCR was performed for CAR and STR primers in individual reactions and were not multiplexed. The amplification conditions were initial denaturing at 94°C for 1 min, followed by 35 cycles of denaturing at 94°C for 25 s, annealing at 53°C for 40 s, extension at 68°C for 40 s, and after all 35 cycles were complete an additional extension phase at 68°C for 5 min. CAR and STR amplicons were analyzed by gel electrophoresis using a 2.5% agarose gel in 1× TAE buffer containing SYBR Safe DNA gel marker (Life Technologies S33102). Amplicons were referenced to 100 bp ladder (NEB #N0467S).

Statistical analysis

Data analysis was performed in R (V.3.2.4) and visualizations created in GraphPad Prism V.10.

RESULTS

Technical validation was aimed at demonstrating analytical validity and reproducibility of the platform as a key component toward development of a sensitive and specific assay. Analytical validity implies the assay is accurate, reproducible, and reliable. This was assessed by concordance between expected and observed spike-in results using the developed IF assays. Performance measurements may be impacted by both antigen expression levels as well as, by antibody specificity and affinity. Two distinct IF assays are necessary to detect (1) the CAR-T cell in peripheral circulation and (2) characterize the B cell phenotype.

Development and technical validation of an HDSCA IF assay for characterization of CD19 targeting CAR-T cells (CAR-T cell assay)

This IF assay was designed to detect rare CAR-T cells from the liquid biopsy at a ratio of 1 CAR-T cell in 3 million normal WCC. Three proprietary antibodies were provided by Kite for CAR detection: KIP-1 (16-6), KIP-3 (14-1), and/or CDL (CD19 CAR FMC63 idiotype antibody; Anti-FMC63 scFv antibody). Each CAR reagent was tested on HDSCA prepared samples consisting of either CAR-T cells or ND cells. IF imaging confirms the localization of the CAR antigen at the membrane, as expected, for all three CAR reagents. CDL (anti-FMC63 scFv) was determined to provide the best separation between CAR-T cells and ND cells using HDSCA prepared samples. As part of the assay development, anti-CD3 (UCHT1) and anti-CD19 (FMC63) were also characterized, and staining

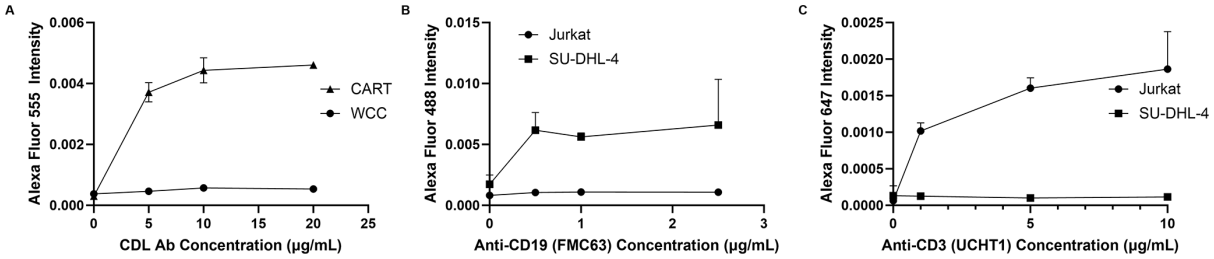

Figure 1 Primary antibody titration for CAR-T cell assay. (A) CDL (anti-id) was added to CAR-T and ND WCC at 0 µg/mL, 5 µg/mL, 10 µg/mL, and 20 µg/mL. (B) Anti-CD19 (FMC63) was added to Jurkat and SUDHL4 at 0 µg/mL, 0.5 µg/mL, 1 µg/mL, and 2.5 µg/mL. (C) Anti-CD3 (UCHT1) direct conjugate to Alexa Fluor 647 was added to SUDHL4 and Jurkat at 0 µg/mL, 1 µg/mL, 5 µg/mL, and 10 µg/mL. n=3. Error bars=SE error. WCC, white cell count.

parameters optimized using SU-DHL-4 and Jurkat cell lines.

Primary antibody titrations were completed for CDL (anti-FMC63 scFv), CD19 (FMC63), and CD3 (UCHT1) directly conjugated to Alexa Fluor 647 (figure 1) using cell lines and ND sample preparations in 12-well slides. The working primary antibody concentrations are CD19 (FMC63) 1 µg/mL, CD3 (UCHT1) 2.5 µg/mL, CDL (anti-FMC63 scFv) 5 µg/mL. Next, using the working primary antibody concentrations, each secondary antibody was titrated to determine the optimal concentration (1:500, 1:1000, 1:2000). The secondary antibodies performed best at 1:500 dilution for all three primary antibodies and were used for all subsequent experiments. The four-color assay consists of DAPI, anti-CD3 (UCHT1) directly conjugated to Alexa Fluor 647, anti-CD19 (FMC63) with Alexa Fluor 488, and CDL (anti-FMC63 scFv) with Alexa Fluor 555. Since the host and isotype matched for CDL and anti-CD3 (both mouse IgG1), these antibodies were introduced at separate steps in which the CDL and anti-mouse Alexa Fluor 555 were incubated first, followed by anti-CD3. The full multiplexed assay was conducted on contrived samples and imaging analysis using automated 100× scanning and 400× manual acquisition indicated good separation between key cellular populations (CD19+vs CD3+CDL+).

Clinical blood samples are processed onto one-well slides for HDSCA analysis. The optimized CAR-T cell assay was further tested in this format to determine the sensitivity of the assay in 3 million cells. Multiplexed staining in the one-well format produced similar staining of contrived samples as in prior experiments. Using OCULAR, we threshold the candidate cells for positivity using the haralick feature sum average (SAV) for the Alexa Fluor 555 channel that corresponds to anti-CDL, which is a weighted intensity metric. A total of 13 candidate CAR-T cells with varying Alexa Fluor 555 SAV values (≥28) and 8 candidate non-CAR WCC were isolated from 4 unique slides to determine the specificity of the CAR-T cell assay at detecting cells with the CAR transgene. Using our nPCR methodology, CAR transgene identification was achieved in 100% of the candidate CAR-T cells (table 2). CAR transgene amplification was specific to CAR-T cells detected in the IF assay as Alexa Fluor 555 (≥28 SAV) and Alexa Fluor 647 positive cells (figure 2A).

The final assay configuration: fixation with 2% neutral buffered formalin solution, blocking with 10% goat serum, primary antibody incubation for CDL (anti-FMC63 scFv) and anti-CD19 (FMC63), secondary antibody incubation with anti-mouse IgG1 Alexa Fluor 555 and anti-mouse IgG2a Alexa Fluor 488, followed with incubation with anti-CD3 (UCHT1) direct conjugation to Alexa Fluor 647. To assess assay linearity and sensitivity, various numbers of CAR-T cells were spiked into normal control blood in triplicates and processed according to the HDSCA workflow.

Table 2 Single cells were isolated from LOD slides and analyzed by nPCR to determine the presence of the CAR transgene

Slide#_Cell#	CAR	Alexa Fluor 555 SAV
1_1	+	60.85
1_2	+	58.79
1_3	+	58.54
1_4	+	57.39
1_8	+	56.21
3_7	+	52.68
3_4	+	49.32
3_5	+	49.32
3_6	+	45.04
1_9	+	43.58
4_1	+	29.32
4_3	+	28.99
4_2	+	28.8
3_1	–	27.02
2_1	–	25.66
3_3	–	25.29
3_2	–	23.34
2_2	–	5.39
1_7	–	2.87
1_6	–	2.35
1_5	–	2.01

The CAR transgene was confirmed in all cells with an Alexa Fluor 555 SAV value of 28 or more. Alexa Fluor 555 SAV sorted by largest to smallest.
LOD, limit of detection; nPCR, nested PCR.

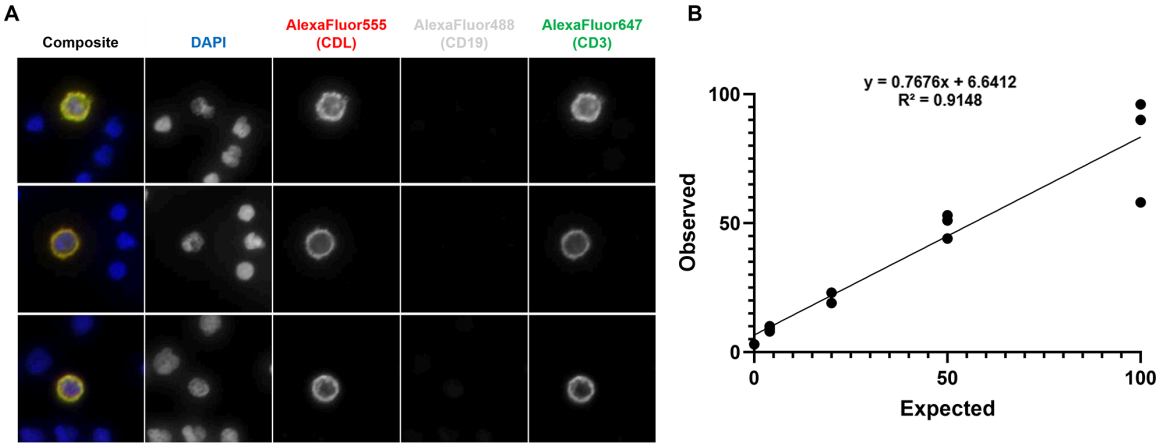

Figure 2 LOD for CAR-T cell assay. ND cells spiked with CAR-T cells at 0, 4, 20, 50, and 100 and stained with CD19 (FMC63, 1 ug/mL: Alexa Fluor 488), CD3 (UCHT1-Alexa Fluor 647, 2.5 µg/mL: Alexa Fluor 647), and CDL (GS anti-ID, 5 µg/mL: Alexa Fluor 555). (A) Gallery of CAR-T cells detected. Images taken at ×400 magnification. (B) Graphical representation of LOD using the CAR-T cell assay and a threshold of CDL positivity of ≥28 Alexa Fluor555 SAV. LOD, limit of detection.

As displayed in figure 2B, mean observed CAR-T cells were plotted against expected CAR-T cells and displayed a correlation coefficient (R^2) of 0.9148.

Genomic nPCR optimization for CAR confirmation

The nPCR protocol has been optimized to confirm the presence of the CAR transgene in single cells (primer sequences provided in table 1). HDSCA stained ND cells and CAR-T cells were collected in bulk for initial testing. All three STR primer pairs worked well on both cell types. We decided to not continue experimentation with STR3, as it sits on the Y-chromosome and would only be applicable to male patients. STR1 was selected as the control to move forward with optimization due to the larger product (486 bp) which is farther in size from the CAR transgene (CAR: 116 bp, STR2: 291 bp). Optimization was completed to ensure the reproducibility of the nPCR approach. Experimental conditions tested: primer concentrations (inner and outer; CAR only), annealing temperature, and the inner amplification input DNA volume.

We performed CAR primer concentration gradients for both outer and inner amplifications. STR primer concentration kept at 0.2 µM throughout. For the outer and inner amplification steps, the CAR primers were tested at. 0.2, 0.3, and 0.4 µM. The 0.4 µM CAR primer pairs performed the best on the outer amplification, while on the inner amplification step both the 0.3 and 0.4 µM performed well (figure 3A). Additionally, the amount of outer amplification PCR product used as template DNA on the inner amplification step was tested (0.5 or 1 µL) and from a qualitative assessment the 1 µL was superior (figure 3B).

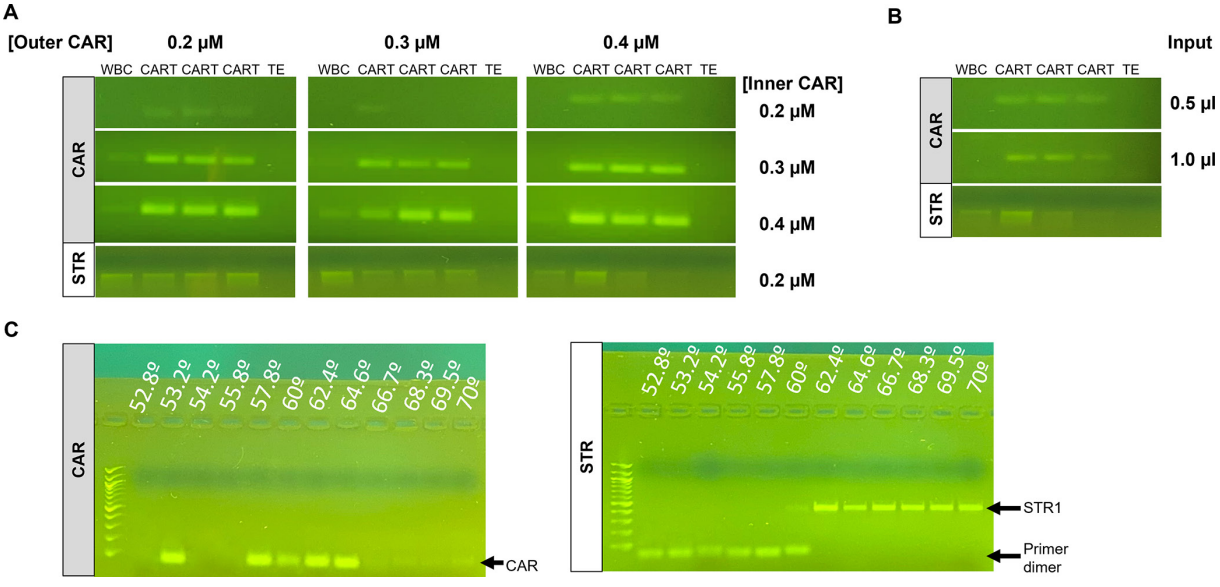

Figure 3 Single cell nPCR methodology for the detection of the CAR transgene. (A) Primer concentration gradient, (B) optimization of template DNA input for inner amplification step, (C) annealing temperature gradient. nPCR, nested PCR; STR, short tandem repeat.

Since the outer amplification step involves multiplexing two primer pairs (CAR and STR1) which have variable estimated melting temperatures (Tm), optimization of the annealing temperature at this step will improve the output of the multiplexed reactions. The outer amplification was conducted with 0.2 µM STR primers and 0.4 µM CAR primers with variable annealing temperature (52.8°C–70°C). The inner amplification step was performed with the CAR (0.3 µM) and STR (0.2 µM) primers as independent runs (not multiplexed) using 1 µL outer amplification product. The results indicate primer dimer formation in the STR product using annealing temperatures of 52°C–60°C, with the most robust band on the gel corresponding to 62.4°C (figure 3C). The CAR product was robust using annealing temperatures 57°C–64°C. The outer amplification annealing temperature for the final protocol was 62°C, which provides robust amplification of CAR and STR amplicons.

The optimized nPCR protocol is presented in the Methods section.

Development and technical validation of B cell assay

This IF assay was designed to detect and analyze CD19 expressing neoplastic cells in PB from anti-CD19 CAR-T cell treated patients. A four-color IF assay has been developed to detect 2 variants of CD19, Clone IDs FMC63 and LE-CD19, and a third biomarker for B cells (either CD20 or CD22). This assay will be referred to as the B Cell Assay. The anti-CD19 (LE-CD19) recognizes the highly conserved C-terminus of CD19, which when combined with anti-CD19 (FMC63) enhances the resolution of the CD19 landscape analysis to the epitope level. Specificity of the neoplastic B cell targeting reagents (primary mAb and secondary mAb) were estimated in a B cell positive control cell line (SU-DHL-4) and a T cell negative control cell line (Jurkat) that do not contain the CD19 antigen.

Initial experiments were conducted on HDSCA 12-well and 3-well slides. Primary antibody titrations were completed for CD19 (FMC63), CD19 (LE-CD19), CD20 (2H7), and CD22 (S-HCL-1) (figure 4). The working primary antibody concentrations are CD19 (FMC63) 1 µg/mL, CD20 (2H7) 5 µg/mL, and CD22 (S-HCL-1) 1.5 µg/mL. CD19 (LE-CD19) is a ready to use antibody and was determined to work well at a 50% dilution. Using the working primary antibody concentrations, each secondary antibody was titrated to determine the optimal concentration (1:500, 1:1000, 1:2000). The secondary antibody performed best at 1:500 dilution for all four antibodies and was used for all subsequent experiments.

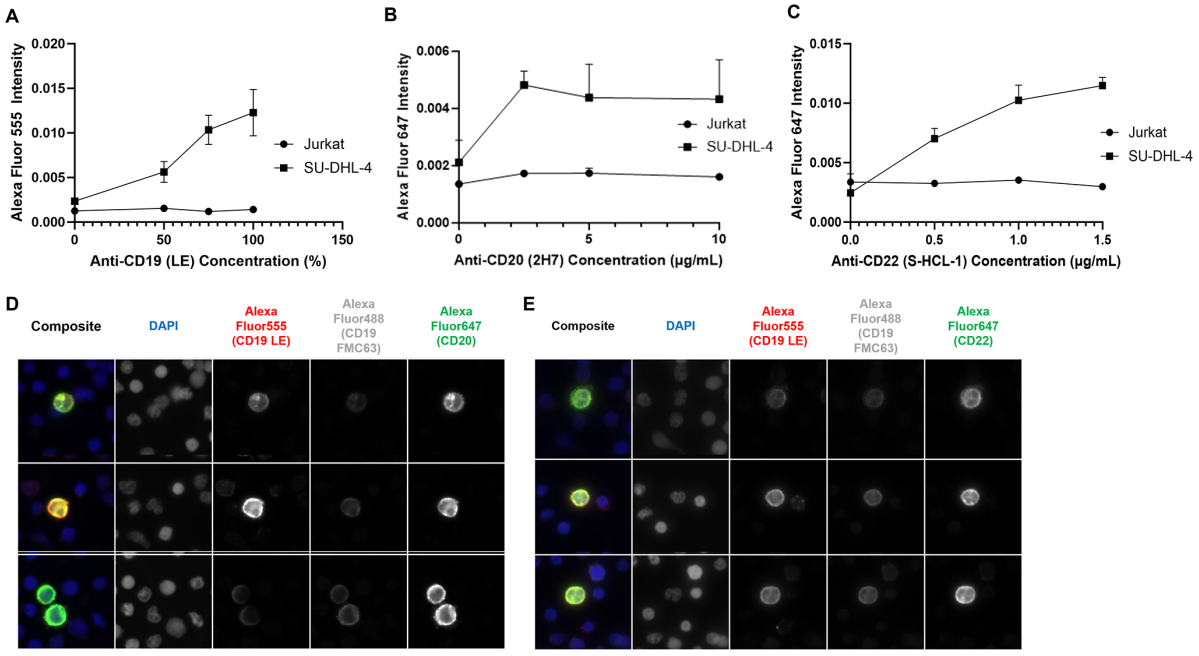

Figure 4 B Cell Assay. (A–C) Optimization of primary antibody concentrations for B cell assay. (A) Anti-CD19 (LE-CD19) was added to SUDHL4 and Jurkat cells at 0, 50, 75, and 100% of the ready to use antibody. Anti-mouse IgG1 Alexa Fluor 555 was used to detect CD19 (LE-CD19) antibody at 1:500 dilution. The final primary antibody concentration for CD19 (LE-CD19) was 50% dilution of the ready to use antibody. (B) Anti-CD20 (2H7) was added to SUDHL4 and Jurkat cells at 0 µg/mL, 2.5 µg/mL, 5 µg/mL, and 10 µg/mL. Anti-mouse IgG2b Alexa Fluor 647 was used to detect CD20 antibody at 1:5000 dilution. The optimal primary antibody concentration for CD20 was 5 µg/mL. (C) Anti-CD22 (S-HCL-1) was added to SUDHL4 and Jurkat cells at 0 µg/mL, 0.5 µg/mL, 1 µg/mL, and 1.5 µg/mL. Anti-mouse IgG2b Alexa Fluor 647 was used to detect CD22 antibody at 1:500 dilution. The optimal primary antibody concentration for CD22 was 1.5 µg/mL. n=3. Error bars=SE error. (D) Multiplex with anti-CD20. ND cells were stained with CD20 (2H7, 5 µg/mL: Alexa Fluor 488), CD19 (FMC63, 1 µg/mL: Alexa Fluor 647), and CD19 (LE-CD19, 50% dilution: Alexa Fluor 555). (E) Multiplex with anti-CD22. ND cells were stained with CD22 (S-HCL-1, 1.5 µg/mL: Alexa Fluor 488), CD19 (FMC63, 1 µg/mL: Alexa Fluor 647), and CD19 (LE-CD19, 50% dilution: Alexa Fluor 555). Images taken at ×400 magnification.

To evaluate specificity of the antibodies, three-well slides with ND cells were used for multiplex staining. The four-color assay consists of DAPI, anti-CD20 (2H7) (figure 4D) or anti-CD22 (S-HCL-1) (figure 4E) with Alexa Fluor 647, anti-CD19 (FMC63) with Alexa Fluor 488, and anti-CD19 (LE-CD19) with Alexa Fluor 555. Imaging analysis using manual acquisition indicated good localization between CD19 antibodies and the CD20 or CD22 antibody. Lastly, the B cell assay was tested in the 1-well slide format using contrived samples, which produced similar staining results as in prior experiments in 12-well and 3-well format. The final assay configuration: fixation with 2% neutral buffered formalin solution, blocking with 10% goat serum, primary antibody incubation, and secondary antibody incubation.

The B cell assay was used on Kite provided ZUMA-3 patient PBMC samples for initial clinical validation of the assay. The patient response and WCC profile are provided in online supplemental file 1. A total of six unique patient samples were provided as cryopreserved PBMCs from the negative fraction of CAR-T manufacturing. We analyzed the DAPI count per slide to determine the adherence per patient sample. There was little variance between sister slides per patient sample, indicating equivalent cell plating per slide. There was a reduced cell count observed for patient 103-012-002 and a higher-than-expected cell count for patient 103-002-012 (online supplemental figure 1).

Analysis of single cells from the ZUMA-3 patient samples indicates high quality membrane localization of the IF signal for all biomarkers. There was a high heterogeneity of B cells detected in the negative fraction samples from the ZUMA-3 cohort (figure 5). Single ($CD19_{FMC63}$+, $CD19_{LE\text{-}CD19}$+, CD20+, or CD22+), double ($CD19_{FMC63}$+$CD19_{LE\text{-}CD19}$+, $CD19_{FMC63}$+CD20+, $CD19_{LE\text{-}CD19}$+CD20+, or $CD19_{LE\text{-}CD19}$+CD22+), and triple ($CD19_{FMC63}$+$CD19_{LE\text{-}CD19}$+CD20+) positive cells were observed. The expression of each biomarker was highly variable on the single cells interrogated and the B cell populations differed between patients (figure 5CG). These results indicate the utility of the B Cell Assay at providing insight into the CD19 landscape of cells in the patients receiving anti-CD19 CAR-T therapy.

DISCUSSION/CONCLUSION

While CAR-T cell therapy is promising for the treatment of B cell malignancies, novel methods to comonitor CAR-T cell presence and performance, together with the cancer cell target epitope landscape, post-treatment, are needed to inform on patient management. More specifically, clinicians are unable to monitor over long intervals CAR-T cell quality or count in individual patients. Rather, indirect measures of CAR-T functionality are taken, such as absolute lymphocyte count, C reactive protein, and ferritin.[32] Similarly, tumor responses are not measured until weeks after infusion, in which the window for further intervention may have closed. To comprehensibly monitor patients proceeding through cellular therapy, longitudinal assessments across the treatment duration are warranted. The liquid biopsy is optimal for this analysis. Prior to therapy, the B cell malignancy itself can be assessed to determine the likelihood of response based on the CD19 landscape and reactivity to the parent antibody used to make the scFv region of the CAR. After infusion post-therapy, further B cell monitoring will determine treatment response and emergence of epitope-loss clones; and CAR-T cell monitoring will determine expansion and function of the therapeutic. If relapse occurs, the patient can be assessed for alternative therapies. For the first time, this study demonstrates the feasibility of this through the use of the HDSCA-HemeCAR platform. Here, we report the technical development, optimization, and validation of multiple IF assays with an approximate LOD of 1 target cell in 3 million, and a single cell genomic assay for CAR-T cell quantification in the liquid biopsy for simultaneous detection of CAR-T cells and the B cell malignancy in patient PB.

The success of adoptive CAR-T cell therapy for cancer has led to the exploration of new indications in solid tumors, autoimmune, and infectious diseases. The most important factors that influence patient outcome and durability of the response are proliferation (peak expansion kinetics) and persistence of the CAR-T cells after infusion.[7 33 34] Given treatment complexity and heterogeneity of cellular expansion, strategies to monitor circulating CAR-T cells in blood samples after treatment are needed. Expansion and persistence of the CAR-T cell population may be critical factors of antitumor efficacy,[35] but CAR-T cells induce two categories of toxicities: (a) general toxicities related to Tcell activation and subsequent systemic release of cytokines and (b) toxicities resulting from ontarget, offtumor effects.[36–38]

Monitoring circulating CAR-T cells in blood samples is currently conducted via flow cytometry or qPCR.[39] These methodologies have limitations in detection sensitivity and single cell analysis capabilities. The enrichment-free strategy used here results in high sensitivity and specificity, while enabling detailed morphological characterization of the target cell population. Here, we have successfully developed an assay for the detection of CAR-T cells from the liquid biopsy with a linear regression (y=07 676x+6.6412) that reports an R^2 of 0.9148 which can be interpreted as a 91% sensitivity observed within the LOD analysis. This shows that the detection of rare CAR-T cells in the liquid biopsy is feasible and can produce comparable sensitivity to previously reported tumor-informed approaches. The HD-CTC assay using a similar methodology previously reported an R^2 of 0.9997,[23] while ctDNA approaches have reported sensitivities of 40%–80% depending on the cancer type and stage.[40] The CAR-T assay demonstrated robust performance in cell lines, which requires further validation in patient samples. The reproducibility and robustness

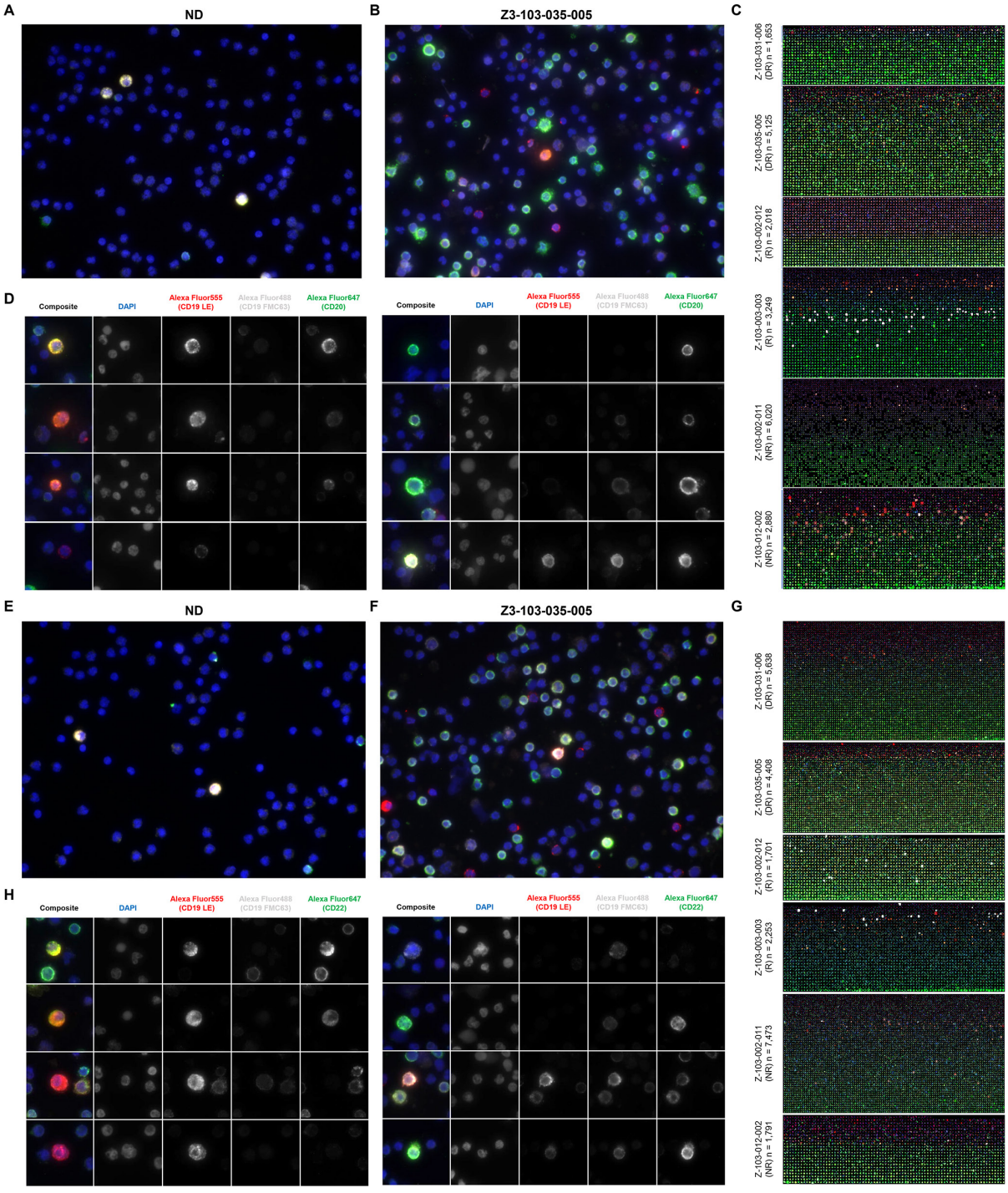

Figure 5 ZUMA-3 patient samples analyzed by the B cell assay (A-D: CD20; E–G: CD22). (A, E) Representative image from an ND PB sample. (B, F) Representative image from a ZUMA-3 patient sample. Images taken at ×400 magnification. (C, G) Gallery of rare cells detected in each ZUMA-3 patient sample, sorted on CD20 (C) or CD22 (G) low to high signal intensity. Images from automated ×100 scanning. DAPI: blue, CD19 (LE-CD19): red, CD19 (FMC63): white, and CD20 or CD22: green. (D, H) Representative gallery of rare cells detected in the negative fractions from the ZUMA-3 cohort. DR, durable response; R, early relapse, NR, no response.

of the IF assay with a semi-quantitative characterization of each cell is critical for our interest in downstream molecular analysis. The identification of CAR signal on the membrane of the T cell also confirms the successful production of the CAR protein and translocation to the membrane. Routine monitoring of CAR-T cell populations may provide insight into the quality, heterogeneity, and persistence of CAR-T cells in circulation, while allowing for association with the occurrence of toxic events.

Genomic analysis was additionally used to confirm the presence of the CAR transgene. The nPCR methodology

was used due to the increased sensitivity and specificity of the assay reaction compared with standard PCR since it involves two primer sets directed against the same target and successive PCR reactions. The main disadvantage of nPCR is the high rate of contamination during transfer of first-round products. Additionally, nPCR is time-consuming and costly as it requires more reagents due to the additional round of PCR required. The nPCR optimized here does show presence or absence of the CAR transgene in a single cell, which was used to technically validate the IF assay.

In subsequent studies the CAR-T cells will be molecularly characterized by single cell genomics and targeted proteomics. Further characterization is needed to understand the copy number profile of the CAR transgene and protein expression profile as we cannot assume correlation of protein quantity to number of genes. It is possible that CAR negative cells by IF may be CAR transgene positive cells unable to express the CAR protein, possibly due to mechanisms such as gene silencing. Furthermore, longitudinal assessment of the CAR-T cells in patient samples can show those CAR-T cells that may have a naturally lower CAR expression, while others decrease their CAR expression over time. Additionally, sequence mapping of the CAR insertion site may provide insight into the functional persisting CAR-T cells based on insertion profile, which would benefit future product development. These types of studies are important to maximize our understanding of therapeutic success or failure, especially given the increase in cell-based therapies.

Monitoring CAR-T cell therapy includes understanding the quality of the host environment, tumor antigen profile, tumor cell response, and anti-CAR immunity which can be conducted via the liquid biopsy. This study additionally developed a single assay to interrogate B cells and report the successful completion of two B cell assays with multiple CD19 variants (FMC63 and LE-CD19) and a unique fourth channel biomarker (CD20 or CD22). The B cell assays assess the CD19 landscape of the patient to understand treatment efficacy and resistance. The epitope for the anti-CD19 CAR-T cell (FMC63 antibody clone) is a conformational epitope spanning exons 3 and 4.[41 42] Alternatively splicing and/or CD19 mutations may lead to loss of the cell surface CAR-binding epitope and thus antigen evasion-mediated relapse, but without impacting the CD19 protein.[17] In the patient samples, we observed that CD19 isoforms were highly heterogeneous in both intrapatient and interpatient. This study was limited by the lack of a large cohort for clinical validation. Here, we show the completion of the technical validation for HDSCA-HemeCAR, we intend to establish the collection of PB samples from patients being treated with KTE-X19 CAR-T cells.

Prior studies have shown the impact of the tumor microenvironment on the efficacy of CAR-T cell therapy, in which CAR-T cell proliferation is inhibited due to an immunosuppressive milieu from the tumor microenvironment, which is unfavorable for antitumor activity.[43] Several factors have been described in the literature. This includes, but is not limited to, anti-inflammatory cytokine secretion (ie, IL-10 and TGFβ) leading to dysfunction of the T cell response, production of chemokines that promote tumor progression via regulatory T cells and myeloid-derived suppressor cell recruitment, platelet–cell interactions, as well as the involvement of tumor associated macrophages, dendritic cells, and fibroblasts.[44–48] The HDSCA workflow has the advantage of downstream proteomic analysis using imaging mass cytometry to further characterize not only the heterogeneity of CAR-T and malignant B cells, but also the tumor microenvironment. Understanding the tumor microenvironment may reveal why CAR-T cells are unable to efficiently kill tumor cells and how the lack of immune cells can lead to treatment failure.[49 50] Targeted multiplex proteomics can provide further detail on anti-CAR-T immunity in survivors and potentially identify which patients would benefit from further immunotherapy versus chemotherapy or alternative treatment options. Additionally, this may provide insight into how to modulation the tumor microenvironment to potentially augment CAR-T cell therapy efficacy for a more durable response.

Author affiliations
[1]Convergent Science Institute in Cancer, Michelson Center for Convergent Bioscience, University of Southern California, Los Angeles, California, USA
[2]Kite A Gilead Company, Santa Monica, California, USA
[3]Department of Biological Sciences Sciences, Dornsife College of Letters, Arts, and Sciences, University of Southern California, Los Angeles, California, USA
[4]Department of Biomedical Engineering, Viterbi School of Engineering, University of Southern California, Los Angeles, California, USA
[5]Department of Aerospace and Mechanical Engineering, Viterbi School of Engineering, University of Southern California, Los Angeles, California, USA
[6]Institute of Urology, Catherine & Joseph Aresty Department of Urology, Keck School of Medicine, University of Southern California, Los Angeles, California, USA
[7]Norris Comprehensive Cancer Center, Keck School of Medicine, University of Southern California, Los Angeles, California, USA

Twitter Peter Kuhn @pkuhn1

Acknowledgements We are grateful to the administrative staff of the CSI-Cancer, Elvia Nunez and Allison Welsh, for their assistance in supporting our research operations.

Contributors Assisted with study concept and design: JR, AB, PK and SNS; Acquired, analyzed, or interpreted the data: SNS, OH, SJ and AM; Provided critical revision of the paper for important intellectual content: AB, JR and SNS; Calculated statistical analysis: SNS; Obtained funding: PK, AB and JR; Provided administrative, technical, or material support: DH and JR; Supervised study: PK and SNS; Guarantor: SNS.

Funding This study was funded by Kite Pharma.

Competing interests PK: founder and Chief Scientific Advisor, and received stock and receiving dividends, Epic Sciences. DH, JR and AB employed by PK. No potential conflicts of interests were disclosed by the other authors.

Patient consent for publication Not applicable.

Provenance and peer review Not commissioned; externally peer reviewed.

Data availability statement All data relevant to the study are included in the article or uploaded as supplementary information. Data are available on reasonable request. Data files and image repository can be accessed through BloodPAC Accession ID: BPDC000139 and the permalink (URL) https://data.bloodpac.org/discovery/BPDC000139.

ORCID iD

Peter Kuhn http://orcid.org/0000-0003-2629-4505

REFERENCES

1 Kochenderfer JN, Dudley ME, Feldman SA, *et al*. B-cell depletion and remissions of malignancy along with cytokine-associated toxicity in a clinical trial of anti-CD19 chimeric-antigen-receptor–transduced T cells. *Blood* 2012;119:2709–20.
2 Maude SL, Frey N, Shaw PA, *et al*. Chimeric antigen receptor T cells for sustained remissions in leukemia. *N Engl J Med* 2014;371:1507–17.
3 Neelapu SS, Locke FL, Bartlett NL, *et al*. Axicabtagene ciloleucel CAR T-Cell therapy in refractory large B-cell lymphoma. *N Engl J Med* 2017;377:2531–44.
4 Schuster SJ, Bishop MR, Tam CS, *et al*. Tisagenlecleucel in Adult Relapsed or Refractory Diffuse Large B-Cell Lymphoma. *N Engl J Med* 2019;380:45–56.
5 Demaret J, Varlet P, Trauet J, *et al*. Monitoring CAR T-cells using flow cytometry. *Cytometry B Clin Cytom* 2021;100:218–24.
6 Haderbache R, Warda W, Hervouet E, *et al*. Droplet digital PCR allows vector copy number assessment and monitoring of experimental CAR T cells in murine xenograft models or approved CD19 CAR T cell-treated patients. *J Transl Med* 2021;19:265.
7 Fraietta JA, Lacey SF, Orlando EJ, *et al*. Determinants of response and resistance to CD19 chimeric antigen receptor (CAR) T cell therapy of chronic lymphocytic leukemia. *Nat Med* 2018;24:563–71.
8 Hirayama AV, Gauthier J, Hay KA, *et al*. The response to lymphodepletion impacts PFS in patients with aggressive non-Hodgkin lymphoma treated with CD19 CAR T cells. *Blood* 2019;133:1876–87.
9 Park JH, Rivière I, Gonen M, *et al*. Long-term follow-up of CD19 CAR therapy in acute lymphoblastic leukemia. *N Engl J Med* 2018;378:449–59.
10 Melenhorst JJ, Chen GM, Wang M, *et al*. Decade-long leukaemia remissions with persistence of CD4+ CAR T cells. *Nature* 2022;602:503–9.
11 Curran KJ, Margossian SP, Kernan NA, *et al*. Toxicity and response after CD19-specific CAR T-cell therapy in pediatric/young adult relapsed/refractory B-ALL. *Blood* 2019;134:2361–8.
12 Gardner RA, Ceppi F, Rivers J, *et al*. Preemptive mitigation of CD19 CAR T-cell cytokine release syndrome without attenuation of antileukemic efficacy. *Blood* 2019;134:2149–58.
13 Gardner RA, Finney O, Annesley C, *et al*. Intent-to-treat leukemia remission by CD19 CAR T cells of defined formulation and dose in children and young adults. *Blood* 2017;129:3322–31.
14 Lee DW, Kochenderfer JN, Stetler-Stevenson M, *et al*. T cells expressing CD19 chimeric antigen receptors for acute lymphoblastic leukaemia in children and young adults: a phase 1 dose-escalation trial. *The Lancet* 2015;385:517–28.
15 Xu X, Sun Q, Liang X, *et al*. Mechanisms of relapse After CD19 CAR T-Cell therapy for acute lymphoblastic leukemia and its prevention and treatment strategies. *Front Immunol* 2019;10:2664.
16 Plaks V, Rossi JM, Chou J, *et al*. CD19 target evasion as a mechanism of relapse in large B-cell lymphoma treated with axicabtagene ciloleucel. *Blood* 2021;138:1081–5.
17 Sotillo E, Barrett DM, Black KL, *et al*. Convergence of acquired mutations and alternative splicing of CD19 enables resistance to CART-19 immunotherapy. *Cancer Discov* 2015;5:1282–95.
18 Chai S, Matsumoto N, Storgard R, *et al*. Platelet-coated circulating tumor cells are a predictive biomarker in patients with metastatic castrate-resistant prostate Cancer. *Mol Cancer Res* 2021;19:2036–45.
19 Shishido SN, Sayeed S, Courcoubetis G, *et al*. Characterization of cellular and acellular analytes from pre-cystectomy liquid biopsies in patients newly diagnosed with primary bladder cancer. *Cancers* 2022;14:758.
20 Armstrong AJ, Halabi S, Luo J, *et al*. Prospective Multicenter Validation of Androgen Receptor Splice Variant 7 and Hormone Therapy Resistance in High-Risk Castration-Resistant Prostate Cancer: The PROPHECY Study. *JCO* 2019;37:1120–9.
21 Scher HI, Graf RP, Schreiber NA, *et al*. Assessment of the Validity of Nuclear-Localized Androgen Receptor Splice Variant 7 in Circulating Tumor Cells as a Predictive Biomarker for Castration-Resistant Prostate Cancer. *JAMA Oncol* 2018;4:1179–86.
22 Scher HI, Lu D, Schreiber NA, *et al*. Association of AR-V7 on Circulating Tumor Cells as a Treatment-Specific Biomarker With Outcomes and Survival in Castration-Resistant Prostate Cancer. *JAMA Oncol* 2016;2:1441–9.
23 Marrinucci D, Bethel K, Kolatkar A, *et al*. Fluid biopsy in patients with metastatic prostate, pancreatic and breast cancers. *Phys Biol* 2012;9:016003.
24 Rodríguez-Lee M, Kolatkar A, McCormick M, *et al*. Effect of Blood Collection Tube Type and Time to Processing on the Enumeration and High-Content Characterization of Circulating Tumor Cells Using the High-Definition Single-Cell Assay. *Arch Pathol Lab Med* 2018;142:198–207.
25 Shishido SN, Welter L, Rodriguez-Lee M, *et al*. Preanalytical variables for the genomic assessment of the cellular and acellular fractions of the liquid biopsy in a cohort of breast cancer patients. *J Mol Diagn* 2020;22:319–37.
26 Thiele J-A, Pitule P, Hicks J, *et al*. Single-Cell Analysis of Circulating Tumor Cells. *Methods Mol Biol* 2019;1908:243–64.
27 Chai S, Ruiz-Velasco C, Naghdloo A, *et al*. Identification of epithelial and mesenchymal circulating tumor cells in clonal lineage of an aggressive prostate cancer case. *NPJ Precis Oncol* 2022;6:41.
28 Setayesh SM, Hart O, Naghdloo A, *et al*. Multianalyte liquid biopsy to aid the diagnostic workup of breast cancer. *NPJ Breast Cancer* 2022;8:112.
29 Shishido SN, Ghoreifi A, Sayeed S, *et al*. Liquid biopsy landscape in patients with primary upper tract urothelial carcinoma. *Cancers* 2022;14:3007:12.:.
30 Ruiz C, Li J, Luttgen MS, *et al*. Limited genomic heterogeneity of circulating melanoma cells in advanced stage patients. *Phys Biol* 2015;12:016008.
31 Malcov M, Schwartz T, Mei-Raz N, *et al*. Multiplex nested PCR for preimplantation genetic diagnosis of spinal muscular atrophy. *Fetal Diagn Ther* 2004;19:199–206.
32 Selim AG, Minson A, Blombery P, *et al*. CAR-T cell therapy: practical guide to routine laboratory monitoring. *Pathology* 2021;53:408–15.
33 Ghorashian S, Kramer AM, Onuoha S, *et al*. Enhanced CAR T cell expansion and prolonged persistence in pediatric patients with ALL treated with a low-affinity CD19 CAR. *Nat Med* 2019;25:1408–14.
34 Qi T, McGrath K, Ranganathan R, *et al*. Cellular kinetics: a clinical and computational review of CAR-T cell pharmacology. *Adv Drug Deliv Rev* 2022;188:114421.
35 McLellan AD, Ali Hosseini Rad SM. Chimeric antigen receptor T cell persistence and memory cell formation. *Immunol Cell Biol* 2019;97:664–74.
36 Bonifant CL, Jackson HJ, Brentjens RJ, *et al*. Toxicity and management in CAR T-cell therapy. *Mol Ther Oncolytics* 2016;3:16011.
37 Maude SL, Laetsch TW, Buechner J, *et al*. Tisagenlecleucel in Children and Young Adults with B-Cell Lymphoblastic Leukemia. *N Engl J Med* 2018;378:439–48.
38 Turtle CJ, Hanafi L-A, Berger C, *et al*. CD19 CAR-T cells of defined CD4+:CD8+ composition in adult B cell ALL patients. *J Clin Invest* 2016;126:85309:2123–38.:.
39 Schanda N, Sauer T, Kunz A, *et al*. Sensitivity and specificity of CD19.CAR-T cell detection by flow cytometry and PCR. *Cells* 2021;10:3208:11.:.
40 Duffy MJ, Diamandis EP, Crown J. Circulating tumor DNA (ctDNA) as a pan-cancer screening test: is it finally on the horizon? *Clinical Chemistry and Laboratory Medicine (CCLM)* 2021;59:1353–61.
41 Klesmith JR, Wu L, Lobb RR, *et al*. Fine Epitope Mapping of the CD19 Extracellular Domain Promotes Design. *Biochemistry* 2019;58:4869–81.
42 Orlando EJ, Han X, Tribouley C, *et al*. Genetic mechanisms of target antigen loss in CAR19 therapy of acute lymphoblastic leukemia. *Nat Med* 2018;24:1504–6.
43 Yan Z-X, Li L, Wang W, *et al*. Clinical Efficacy and Tumor Microenvironment Influence in a Dose-Escalation Study of Anti-CD19 Chimeric Antigen Receptor T Cells in Refractory B-Cell Non-Hodgkin's Lymphoma. *Clin Cancer Res* 2019;25:6995–7003.
44 Ruffell B, Chang-Strachan D, Chan V, *et al*. Macrophage IL-10 blocks CD8+ T cell-dependent responses to chemotherapy by suppressing

IL-12 expression in intratumoral dendritic cells. *Cancer Cell* 2014;26:623–37.
45 Seo N, Hayakawa S, Takigawa M, *et al*. Interleukin-10 expressed at early tumour sites induces subsequent generation of CD4(+) T-regulatory cells and systemic collapse of antitumour immunity. *Immunology* 2001;103:449–57.
46 Shah NN, Fry TJ. Mechanisms of resistance to CAR T cell therapy. *Nat Rev Clin Oncol* 2019;16:372–85.
47 van der Woude LL, Gorris MAJ, Halilovic A, *et al*. Migrating into the Tumor: a roadmap for T cells. *Trends Cancer* 2017;3:797–808.
48 Yan M, Jurasz P. The role of platelets in the tumor microenvironment: from solid tumors to leukemia. *Biochim Biophys Acta* 2016;1863:392–400.
49 Scholler N, Perbost R, Locke FL, *et al*. Tumor immune contexture is a determinant of anti-CD19 CAR T cell efficacy in large B cell lymphoma. *Nat Med* 2022;28:1872–82.
50 Spiegel JY, Patel S, Muffly L, *et al*. CAR T cells with dual targeting of CD19 and CD22 in adult patients with recurrent or refractory B cell malignancies: a phase 1 trial. *Nat Med* 2021;27:1419–31.

Supplemental Material

Supplemental Table 1. Primer sets used for nPCR for CAR transgene detection at the single cell level.

Primer Name		Sequence	Tm (ºC)	Product size (bp)
STR1 (chr5)	Forward	TTGCAGGAAATGCTGGCATAGAGC	68.5	486
	Reverse	TTCTGTAACATTTTGCCACATACGCC	66.8	
STR2 (chr5)	Forward	TGCAGCCTAATAATTGTTTTCTTTGGG	66	291
	Reverse	AGATTCACTTTCATAATGCTGGCAGA	64.3	
STR3 (chrY)	Forward	ACCACTGTACTGACTGTGATTACAC	57.3	495
	Reverse	GCACCTCTTTGGTATCTGAGAAAGT	61.3	
CAR (outer)	Forward	TCAGGGGTCTCATTACCCGA	57.4	717
	Reverse	ATCGTACTCCTCTCTTCGTCCT	56.6	
CAR (inner)	Forward	GCCATTTACTACTGTGCCAAAC	54.5	116
	Reverse	GGATACATAACTTCAATTGCGGC	54.5	

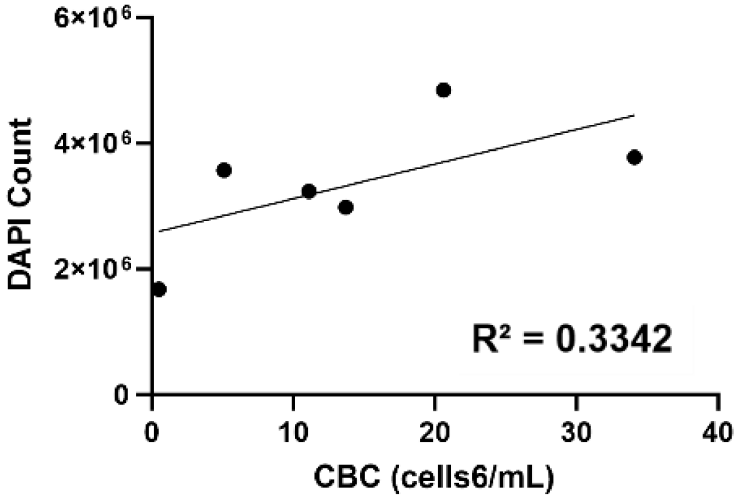

Supplemental Figure 1. ZUMA-3 patient sample cell adherence. Correlation plot of total WBC count per cryopreserved sample and DAPI count per slide.

Supplemental Table 2. ZUMA-3 patient sample information. *CBC count taken as a 10ml cellular suspension in PBS.

Patient #	Response	WBC e6/ml*	LYM%	MID%	GRA%
Z3-103-002-012	Early Relapse	20.6	80.4	15.0	4.6
Z3-103-012-002	Primary Refractory	0.5	60.4	6.9	32.7
Z4-103-003-003	Early Relapse	13.7	59.4	27.4	13.2
Z3-103-035-005	Durable Response	5.1	84.7	8.6	6.7
Z3-103-031-006	Durable Response	11.1	78.6	18.1	3.3
Z3-103-002-011	Primary Refractory	34.1	75.9	19.1	5